Brazilian Journal of Physics (2024) 54:200
https://doi.org/10.1007/s13538-024-01571-2

Development of Metamaterial Using Waste Materials for Microwave Absorption

Deeksha Gupta[1] · Prabhakar Kumar[1] · Ashish Dubey[2] · Abhishek Kumar[1]

Received: 8 May 2024 / Accepted: 29 July 2024 / Published online: 14 August 2024

Abstract
The present study focuses on the use of waste materials to generate cost-effective microwave absorption composites. Rice husk (agricultural waste) and exhausted activated charcoal (water filter cartridge waste) were used as waste materials for microwave absorption. Both were blended in different proportions using a planetary ball mill to prepare samples. The XRF and particle size studies were carried out for element and particle size analysis, and for dielectric properties measurement, a vector network analyzer was used. The findings reveal the microwave absorption in the frequency range of 2 to 18 GHz by the blended composites. Sample RHC-11 with 20% exhausted activated charcoal showed a maximum reflection loss of − 38.3 dB at 12 GHz. For further improvement in microwave absorption, the dielectric characteristics of the composites were utilized to develop a layered metamaterial-based microwave absorber. The layered metamaterial is a unique and simple patch design that displays good microwave absorption > 90% and absorbs 99.34% of microwave energy at 16 GHz frequency. The developed metamaterial-based microwave absorber shows an absorption bandwidth of 6.60 GHz with a thickness of 2.3 mm. In addition, the proposed structure is independent of the oblique incidence angle and polarization angle.

Keywords Exhausted activated carbon (EAC) · Metamaterial · Microwave absorber · Reflection loss · Rice husk

1 Introduction

The development and use of electronic equipment give rise to electromagnetic pollution. The increasing rate of electromagnetic pollution has highlighted the need for materials that can absorb electromagnetic waves without hindering equipment functionality and harming human health [1]. For designing microwave absorber, dielectric and magnetic properties are required. Commonly used materials for microwave absorption include ferrites, metal powders (such as Fe, Ni, and Co), and alloys. However, these materials have limitations, such as high density and chemical activity [2, 3]. Other than these conventional microwave-absorbing materials, carbon material possesses a high microwave absorption capacity [4, 5].

In the past few years, researchers came up with the idea of designing microwave absorbers using agricultural waste materials such as rice husk, banana leaves, corn husk, walnut shells, and mango leaves [6]. Rice husk is the agricultural waste materials produced in large quantities from the rice milling process. It is typically burned in the field which potentially creates environmental issues and major challenges. Wu et al. [1] prepared a biomass hierarchical porous structure using carbon, which is achieved from rice husk using KOH activation and resulted in a minimum reflection loss of − 47.47 dB at 9.79 GHz with a sample thickness of 2.8 mm. Negi et al. [6] used a two-step carbonization process to synthesize mango leaves to obtain activated carbon, which gives 5.17 GHz of effective bandwidth at 1.75 mm thickness, covering 86.61% of the K_u band, and 3.31 GHz of bandwidth at 2.5 mm material thickness, absorbing about 82.75% of the X-band. Mishra et al. [7] fabricated rice husk bio-composites using the green method, i.e., without burning rice husk. Their electromagnetic parameters showed that the dielectric constant decreases with an increase in frequency. The result obtained by the authors showed that the loss tangent reaches the highest value of 0.31 at a frequency of

✉ Abhishek Kumar
abhishek@mnnit.ac.in

[1] Motilal Nehru National Institute of Technology Allahabad, Prayagraj 211004, India

[2] Defence Materials and Stores Research and Development Establishment, Kanpur, India

12.2 GHz and the lowest value of 0.21 at a frequency of 8.2 GHz. Lee et al. [8] used rice husk ash with polyester and simulated a reflection loss of − 28.40 dB using CST software, which takes place at 13.81 GHz (80% RHA sample) and 90% or more absorption in a bandwidth of 13.44–14.23 GHz and 17.28–18 GHz.

Metamaterial absorbers (MMA) have been the subject of extensive research for a variety of real-time applications such as reduction in Radar cross-section (RCS), electromagnetic interference shielding, and so on [9]. Researchers conducted numerous tests and simulations to develop metamaterials as microwave absorbers with the goal of producing thin, high-absorption-bandwidth, and polarization-insensitive absorbers. The substrate materials and their layering, patch materials, and patch design structures were all varied in the trials. Nasab et al. [10] produced a microwave absorber utilizing A4 copy paper as the substrate with a thickness of 7.2 mm, resulting in 0.4 GHz absorption bandwidth. The thickness of the absorber is one of the most essential concerns when making microwave absorbers, since it limits their use in armor due to increasing weights. In 2014, Yuan et al. [11] produced a 5 mm-thick FR4-based substrate with a 2.46 GHz bandwidth and absorption of more than 90%. When the substrate thickness was reduced to 4.5 mm using FR4 material, the absorption bandwidth was increased to 4.2 GHz. Panwar et al. [12] used Al and Fe_3O_4-Ti to multi-layer the substrate, resulting in a total thickness of 3.4 mm and a 4.2 GHz absorption bandwidth. Chen et al. [13] used F_4B-2 as substrate material with a thickness of 3 mm, which produced a bandwidth of 3.8 GHz. Khan et al. [14, 15] reduced the substrate thickness to 2.4 mm using FR4 material in 2018 and 2017 with different patch designs, resulting in absorption bandwidths of less than 2 and 4 GHz, respectively. This finding demonstrates that the metamaterial microwave absorber's absorptivity is also influenced by patch design. Feng et al. [16] worked on a FeSiAl alloy material; the designed FeSiAl metamaterial exhibits a − 10 dB absorption bandwidth from 4 to 8 GHz and 10 GHz to 15 GHz, and it is sensitive at large incidence angles but not sensitive within 45°. Hussain et al. [17] investigated a graphene-based metamaterial absorber on an FR4 substrate to achieve broadband absorption, with a total thickness of 3.05 mm, showing absorption of more than 50% from 8 to 19 GHz and polarization insensitivity up to 90°.

The aim of the present work is to create a microwave-absorbent composite out of waste materials (rice husk and exhausted activated coal). The phase, particle size, and electromagnetic properties of the waste material were studied using characterization and dielectric testing. Further, a metamaterial structure based on waste-based composites, along with FR4 as a substrate and patch design, has been presented. The applicability of this metamaterial in microwave absorption performance was investigated using HFSS modeling to create an optimal structure with good microwave absorption bandwidth and polarization insensitivity.

2 Materials and Process

The rice husk was thoroughly washed to remove dust and any other contaminants, followed by drying in the oven for 5 h at 80 °C. To acquire exhausted activated coal (EAC), old water filter cartridges are used. The EAC was extracted from an exhausted water filter cartridge and dried in an oven for 5 h at 120 °C to remove any moisture content. To make fine powder of the waste materials, the dry ball milling technique was applied. Both waste materials were separately milled using a planetary ball mill with a 10:1 ratio by weight of steel balls and material. Steel balls were taken in the size ratio of 1:2:4:8, consisting of 18 mm, 15 mm, 8 mm, and 7 mm balls, respectively. The rice husk was milled at 250 rpm for 2 h, and EAC was milled at 300 rpm for 9 h. The resulting fine powder from each material was then kept in an airtight container for further use. Coaxial samples were prepared for the electromagnetic properties. The entire process is summarized in Fig. 1. Sixteen samples were created, varying the EAC concentration from 2 to 30% by weight, and the sample codes are listed in Table 1. A 10:1 ratio of epoxy to hardener was used as a binder.

3 Characterization and Dielectric Property Measurement

X-ray fluorescence (XRF) was carried out for elements present in the rice husk using ProSpector LE. A microtrac nanoparticle size analyzer determined the particle size analyses of powdered samples. Prepared coaxial samples with dimensions (inner diameter = 3.08 mm; outer diameter = 6.9 mm)

Fig. 1 The sample preparation process for making samples

Table 1 Composition of sample prepared with sample codes

S. no	Sample code	EAC (wt.%)	Rice hush (wt.%)
1	RHC-1	0	100
2	RHC-2	2	98
3	RHC-3	4	96
4	RHC-4	6	94
5	RHC-5	8	92
6	RHC-6	10	90
7	RHC-7	12	88
8	RHC-8	14	86
9	RHC-9	16	84
10	RHC-10	18	82
11	RHC-11	20	80
12	RHC-12	22	78
13	RHC-13	24	76
14	RHC-14	26	74
15	RHC-15	28	72
16	RHC-16	30	70

Table 2 Elemental composition of rice husk

S. no	Element	Fraction (ppm)
1	Si	36,000 ± 2200
2	Fe	6000 ± 300
3	K	5800 ± 400
4	Ca	1310 ± 110
5	Mn	830 ± 50
6	Cu	650 ± 40
7	Cr	386 ± 24
8	Ni	374 ± 21
9	Ti	190 ± 30
10	Zn	62 ± 4

were used to determine the relative complex components of permittivity and permeability using a vector network analyzer (VNA). The samples were made by a uniform distribution of the mixture (Rice husk-EAC) at 80% by weight and the binder at 20% by weight.

4 Results and Discussion

4.1 Elemental Analysis

The elemental composition of pure rice husk powder characterized using XRF is shown in Table 2. Silicon is the major component found in the rice husk, followed by iron and potassium.

4.2 Particle Size Analyses

For particle size analyses, powdered rice husk and EAC were dispersed in the solvent and sonicated at 50 Hz for uniform dispersion of powder in the solvent and to prevent agglomeration. The average particle size of pure rice husk and EAC was found to be 57.9 nm and 0.9 nm, respectively.

4.3 Dielectric Properties

The microwave absorption properties of materials depend on their dielectric properties. Dielectric properties are relative permittivity(ε_r) and relative permeability(μ_r) [18].

$$\varepsilon_r = \varepsilon' + \mathrm{i}\,\varepsilon'' \tag{1}$$

$$\mu_r = \mu' + \mathrm{i}\,\mu'' \tag{2}$$

In 0the above equation, the real component of the complex permittivity (ε') and the real component of the complex permeability (μ') are related to a material's ability to store electromagnetic energy, respectively. The ε'' and μ'' 111101 represent the imaginary components of the complex permittivity and complex permeability, respectively, which depicts the ability of the material to dissipate electromagnetic energy, i.e., conversion of stored or absorbed electromagnetic energy into heat energy [19, 20]. The dielectric loss tangent is ($\mathrm{Tan}\delta_e$) is the ratio of complex permittivity's imaginary (ε'') and real parts (ε') as expressed in the equation below.

$$\mathrm{Tan}\ \delta_e = \frac{\varepsilon''}{\varepsilon'} \tag{3}$$

Figure 2 shows the dielectric parameters (ε', ε'', $\mathrm{Tan}\delta_e$) of the prepared composite measured between 2 and 18 GHz. It is observed from Fig. 2 that ε', ε'' and $\mathrm{Tan}\delta_e$ of pure rice husk (RHC-1) show the lowest value among all the samples. The real part of permittivity (ε') increases with an increase in EAC content from 0 to 30% and accordingly, the absorption capacity increases. The imaginary part (ε'') shows that the value decreases on higher frequencies, among all 20% of the EAC content sample shows that as the frequency increases its value also increases and gives the highest value at higher frequency side and 10% and 12% EAC content shows highest value at lower frequency, indicating that it can convert the maximum amount of absorbed microwave energy into heat energy at higher frequencies in comparison with other samples. The curve in $\mathrm{Tan}\delta_e$ shows a similar nature to that of the ε'' and consequently (sample containing 10%, 12%, and 20% EAC) shows the best dielectric loss capacity.

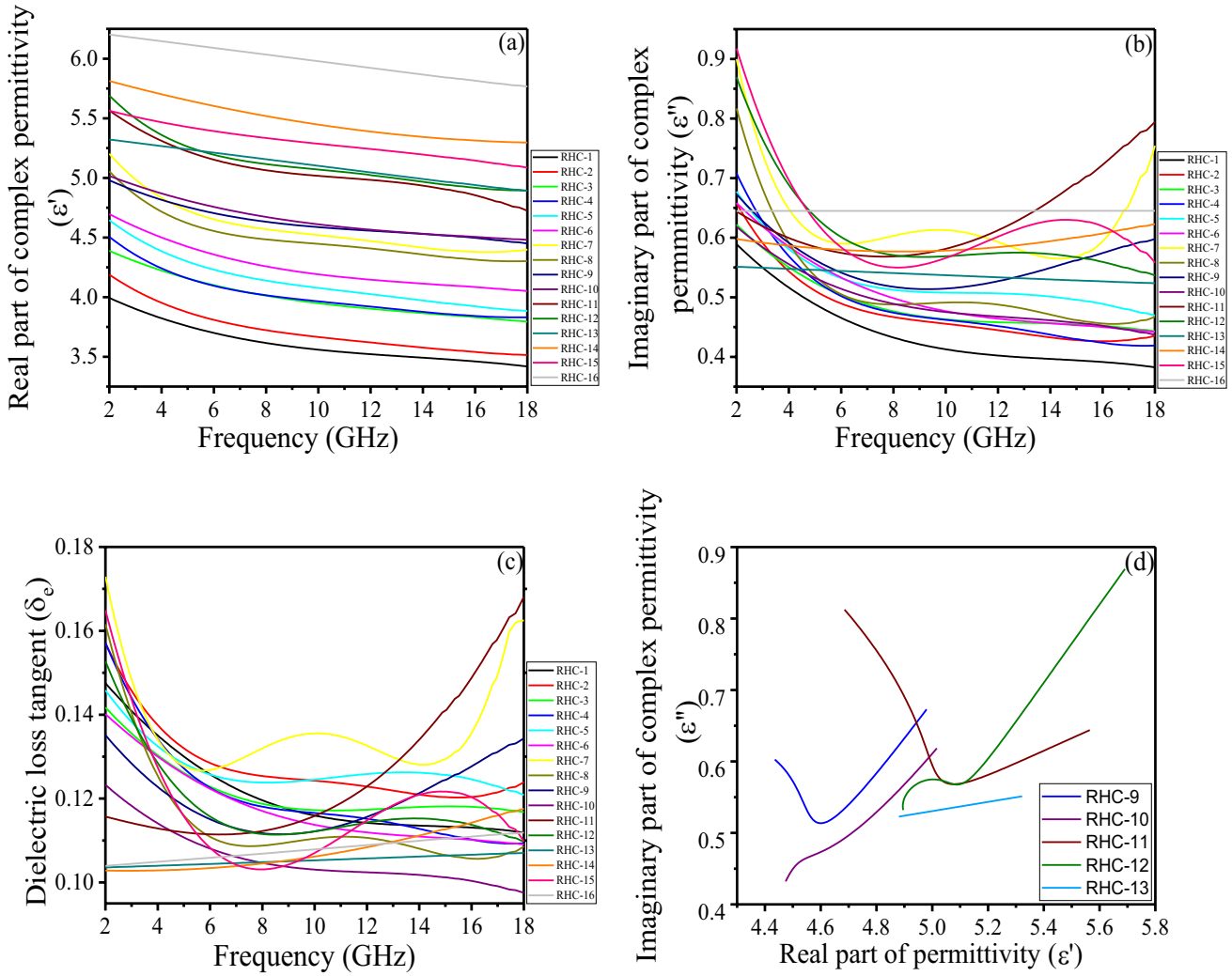

Fig. 2 Dielectric properties of rice husk and EAC composites with different EAC percentages: **a** real part of complex permittivity, **b** imaginary part of complex permittivity, **c** dielectric loss tangent, and **d** Cole-Cole plot

Cole-Cole curves are the effective tool for analyzing and quantifying the polarization relaxation process. Cole-Cole curves are plotted as ε' against ε'', and their mathematical formula is shown in the equation below.

$$\varepsilon' - \left(\frac{\varepsilon_s + \varepsilon}{2}\right)^2 + \varepsilon''^2 = \left(\frac{\varepsilon_s - \varepsilon}{2}\right)^2 \tag{4}$$

where ε_s is the stationary dielectric constant and ε is the relative dielectric constant. The Cole-Cole graphs of a few selected samples are depicted as circles, or more precisely, semicircles in Fig. 2d. Each semicircle in Fig. 2d represents a Debye relaxation process [21]. More number of semi-circles in a system represents a higher number of Debye relaxation processes with higher dielectric polarization. As a result, increased dielectric relaxation translates to increased microwave absorption. In Fig. 2d, there is one large semicircle of sample RHC-11, two small semi-circles of sample RHC-12, and one small semi-circle of sample RHC-9, and the other two show almost a straight line. Possibly, the dominant dielectric loss is the conduction loss due to the EAC content and long tails (straight lines) [22] seen in the cole-cole curves.

The dielectric properties of the absorber significantly impact its electromagnetic wave absorption characteristics [21]. The below reflection loss (RL) formula can be used to calculate the amount of electromagnetic wave absorption).

$$RL = -20\log\left|\left(z_{in} - z_o\right)\right| / \left(z_{in} - z_o\right)| \tag{5}$$

$$z_{in} = z_o\left(\mu_r/\varepsilon_r\right)^{\frac{1}{2}} \tanh\left\{j.\left(\frac{2\pi ft}{c}\right)\left(\mu_r.\varepsilon_r\right)^{\frac{1}{2}}\right\} \tag{6}$$

where μ_r, ε_r are the complex permeability and complex permittivity, f is the frequency, c is the velocity of light, t is the material thickness, z_{in} is the characteristic impedance of absorber, and z_o is the characteristic impedance of free space. The reflection loss (RL) was assessed using MATLAB code for a range of samples, varying in exhausted activated charcoal (EAC) content from 0 to 30%. The measurement frequency ranged from 2 to 18 GHz. The results of a few selected samples (RHC-9, RHC-10, RHC-11, RHC-12, and RHC-13) with the most promising outcomes are depicted in Fig. 3. Additionally, different sample thicknesses, ranging from 1 to 16 mm, were evaluated, and it was found that achieving > 90% absorption (− 10 dB) required a thickness of at least 11 mm. Figure 3a–e shows the reflection loss curves of five samples (RHC-9, RHC-10, RHC-11, RHC-12, and RHC-13) with thicknesses of 12, 14, and 16 mm and frequencies from 2 to 18 GHz. The experimental results for all the samples, along with the optimal outcomes, are summarized in Table 3. Notably, sample RHC-11, containing 20% EAC, exhibited the highest reflection loss of − 38.3 dB at a thickness of 14 mm.

This study focuses on investigating the electromagnetic properties of exhausted activated charcoal and rice husk composites for potential applications in electromagnetic interference (EMI) shielding or absorption. The results demonstrate how varying EAC content and sample thickness affect the reflection loss performance at different frequencies. The application for such thick absorbers is anechoic chambers, which create a controlled electromagnetic environment for accurate antenna and wireless device testing. These absorbers are meticulously applied to line the chamber's walls, ceiling, and floor. The chosen thickness enables effective absorption of incident electromagnetic waves, minimizing reflections within the chamber. As a result, the environment becomes low in reflection, ensuring that any signals emitted or received by devices under test remain free from contamination caused by reflections from the chamber's surfaces.

To further reduce the composite thickness, the dielectric results were utilized to design a metamaterial structure. The structure was simulated using high-frequency structure simulator (HFSS) software to simulate and analyze the electromagnetic properties and performance of the metamaterial structure. Through this simulation process, the unique

Table 3 Maximum reflection loss comparison of selected sample

Samples	Reflection loss (dB)	Matching frequency (GHz)	Thickness (mm)
RHC-9	− 18.6	14.7	12
RHC-10	− 32.7	17.8	14
RHC-11	− 38.3	12.0	14
RHC-12	− 30.4	14.1	12
RHC-13	− 24.5	10.4	16

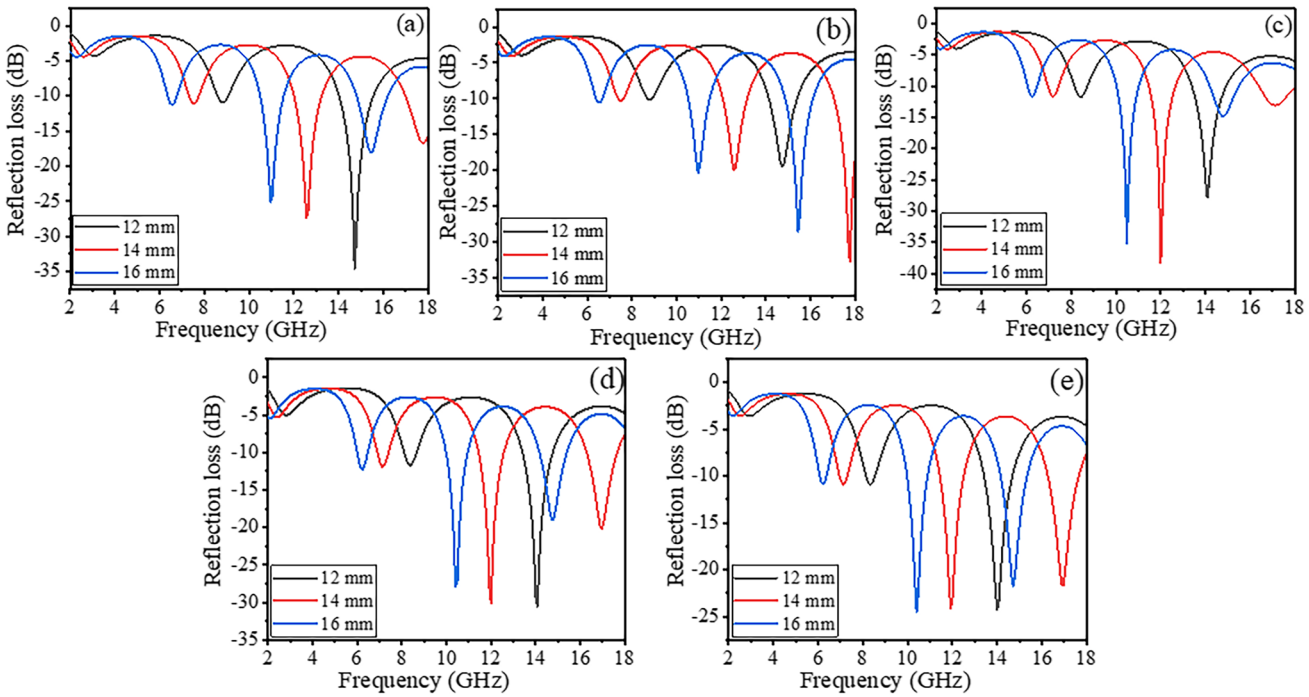

Fig. 3 Reflection loss of rice husk and EAC composites with different EAC percentages: **a** RHC-9, **b** RHC-10, **c** RHC-11, **d** RHC-12, **e** RHC-13

capabilities of metamaterials, aiming to efficiently manipulate and absorb electromagnetic waves were explored. The HFSS software played a critical role in predicting and optimizing the behavior of metamaterial structure, opening up possibilities for applications in various fields that require lightweight and compact electromagnetic absorbers.

5 Metamaterial Design

The design inspiration for this project was drawn from Ghosh et al.'s research [23], where the investigation of a swastika-like structure printed on an FR-4 substrate. This structure exhibited an impressive absorption rate of approximately 99.64% at 10.10 GHz, along with about 81% absorption for incident angles and polarization angles up to 60 degrees. In this work, the aim was to simplify the design to enhance its machinability and reduce its complexity while striving to improve upon the absorption performance and polarization insensitivity. Figure 4 depicts the unit cell of the suggested square-shaped metamaterial microwave absorber design. The pattern consists of three layers, each with a different material: Copper, Rice husk-charcoal mixture, and FR4 Epoxy. The patch is developed on the third layer using Resistive ink. The thin copper film with a thickness of 0.017 mm serves as the background base. Above it, a layer of Rice Husk charcoal mixture, optimized to a thickness of 2 mm is placed and FR4 epoxy is deposited above the mixture with an optimized thickness of 0.3 mm, referred to as layers 2 and 3, respectively. The dielectric properties of the rice husk-charcoal mixture have been taken from the experiment results as discussed in the previous section, which are frequency dependent. The dielectric constant and dielectric loss

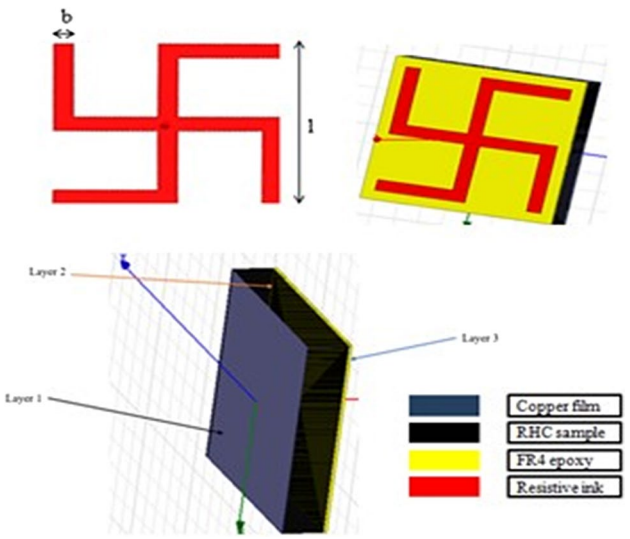

Fig. 4 Schematic structure of proposed absorber unit cell

Table 4 Property of conductive material used

Material	Electrical conductivity, σ(S/m)
Copper (Cu)	5.8×10^7
HSF-71 resistive ink	664

tangent ($Tan\delta_e$) for FR4 epoxy are 4.4 and 0.02, respectively. The conductivity of copper and the resistive ink is tabulated in Table 4 [24, 25].

The dimensions of the Swastika design were optimized using HFSS. This design is proposed considering the following challenges: machinability to reduce the machining time of printing, affordability, wide absorption bandwidth, and polarization-insensitive to efficiently absorb microwave across a broad range of incident angles. All the optimized parameters and dimensions used in the design are tabulated in Table 5. The width of the patch is constant throughout the analyses as shown in Fig. 4.

5.1 Simulation Result and Discussion

The HFSS was used to analyze and model the proposed microwave absorber design with normal and different incidence angles and TE and TM polarization angle. In the simulation, master and slave boundary conditions were used, and excitation was provided by a Floquet port in the XY plane (*Z*-direction). HFSS was used to determine the frequency-dependent dielectric properties of the Rice husk-EAC mixture.

The absorptivity Eq. (7) is being used to calculate the absorption coefficient of the structure [13].

$$A(\omega) = 1 - R(\omega) - T(\omega) \tag{7}$$

In the above equation, $A(\omega)$ = absorptivity, $R(\omega)$ = reflectivity, and $T(\omega)$ = transmissivity. To achieve the highest absorptivity, the reflectivity and transmissivity should be kept to a minimum. The goal of using copper as the ground

Table 5 Optimization dimensions of the design

S. no	Parameter	Dimension (mm)
1	Length of the unit cell (a)	16
2	Thickness of copper film (layer 1) (t_1)	0.017
3	Thickness of layer 2 (t_2)	2
4	Thickness of layer 3 (t_3)	0.3
5	Thickness of patch (t_p)	0.05
6	Length of patch (l)	5.75
7	Width of patch (b)	1.2

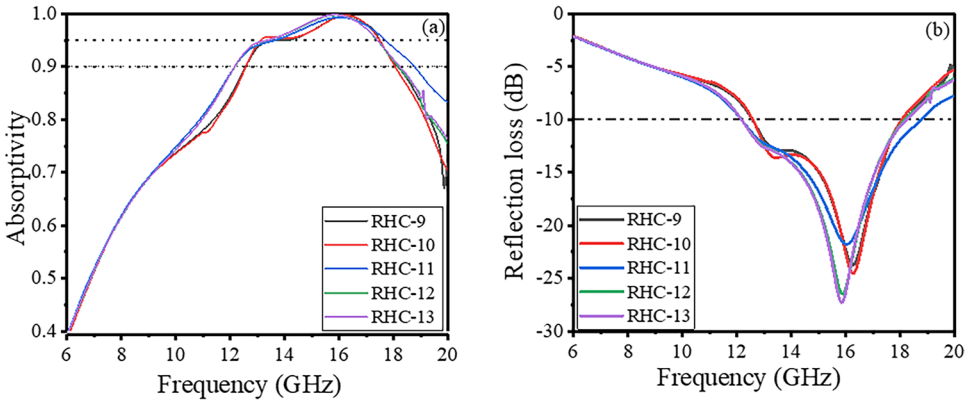

Fig. 5 Absorption (**a**) and reflection loss (**b**) of design using sample RHC-9 to RHC-13

layer is to reduce incident wave transmission to zero. As a result, the absorptivity equation shifts as shown in Eq. (8).

$$A(\omega) = 1 - R(\omega) \tag{8}$$

The reflection coefficient in terms of *S*-parameters is formulated as in Eq. (9).

$$R(\omega) = |S11(\omega)|^2 \tag{9}$$

So, Eq. (8) modified to Eq. (10).

$$A(\omega) = 1 - |S11(\omega)|^2 \tag{10}$$

The absorptivity of the proposed design using all the samples of RHC is simulated in Ansoft HFSS. All experimental samples of RHC were used at layer 2, and the thickness used was 2 mm. The second layer consists of FR4 epoxy with a thickness of 0.3 mm. A few selected results from the simulation have been shown in Fig. 5. From the simulation result, it was seen that the absorption bandwidth using the RHC samples for the proposed design initially increases from RHC-1 to RHC-11 and reaches its highest at RHC-11, which contains 20% EAC in the Rice husk, and then the bandwidth starts decreasing from RHC-12 to RHC-16. This shows that carbon is important in microwave absorption because as the carbon content in EAC increases, the absorption increases as well. However, there is a limit to carbon that can be added to the mixture because, after a certain level of carbon, the absorption reaches its maximum and then begins to decrease. Figure 5 depicts the proposed design's reflection loss and absorptivity using the sample from RHC-9 to RHC-13 placed as the second layer. For all samples, the curve pattern for absorptivity and reflection loss is the same. The sample RHC-11 achieves the greatest results, with absorption greater than 90% and a higher bandwidth. Reflection loss with a value of -10 dB has an absorptivity of 90%, at lower reflection values, the higher the absorptivity. Therefore, metamaterial with sample RHC-11 shows the best results for the reflection loss and absorption bandwidth with absorptivity > 90%. The optimum absorption of the microwave absorber is achieved at RHC-11 (20% EAC content) with an absorption bandwidth (absorptivity > 0.90) of 6.61 GHz between 12.16 and 18.76 GHz. The maximum absorptivity reached is 99.34% at 16 GHz, and the bandwidth with absorptivity greater than 0.95 is 4.02 GHz from 13.38 to 17.40 GHz as shown in Fig. 5. The multilayer construction, consisting of copper which contributes to ohmic losses, FR4 for dielectric losses, and a composite of rice husk and charcoal for additional dielectric losses and conduction losses, effectively strengthens absorption efficiency across a wide range of microwave frequencies. Different layers and having distinct absorption mechanisms might result in absorption bands that overlap. Each individual layer may possess distinct resonance frequencies and bandwidths, which collectively contribute to a more extensive absorption spectrum.

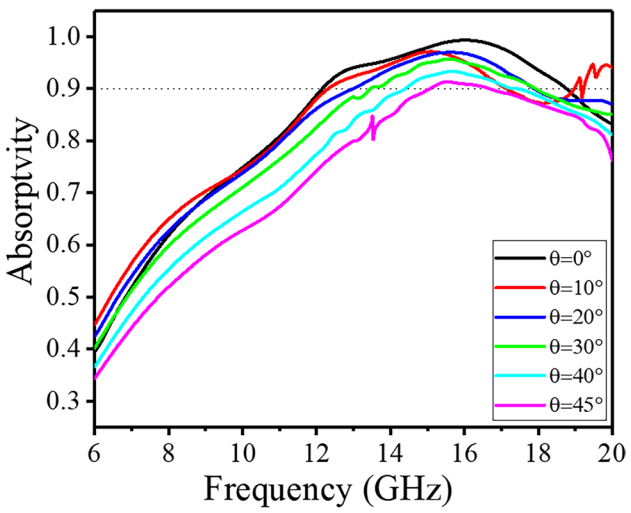

Fig. 6 Absorptivity under oblique incidence angle (θ) of sample RHC-11

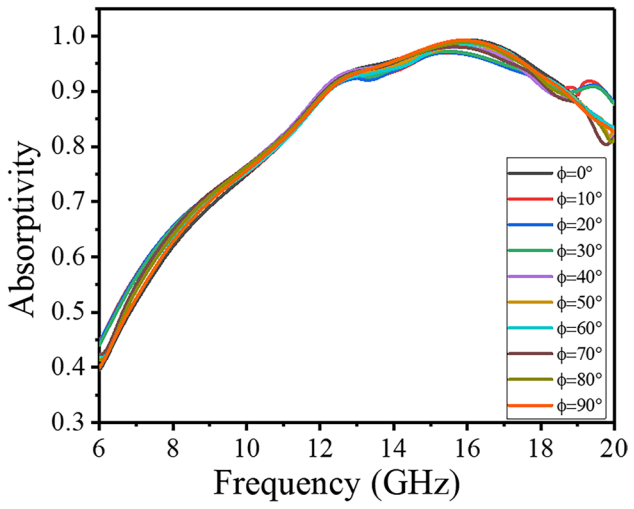

Fig. 7 Absorptivity under different polarization angles (φ) of sample RHC-11

5.2 Absorptivity Under Different Angle Parameters

To check the polarization characteristics of the suggested design for sample RHC-11, a study was conducted by varying the incidence angle (θ) of the wave from 0 to 45° (step size of 10°, from 0 to 40°, then by 5°) and different polarization angles (φ) from 0 to 90° (step size of 10°). When the incidence angle is normal to the surface, the electric field (*E*) and magnetic field (*K*) are parallel to the *x* and *y*-axis, respectively, and the wave propagates perpendicular to the patch design in the *z*-direction. Incident waves which are falling perpendicularly on the patch design are having incidence angle (θ) equal to 0°, while waves parallel to the design have an incidence angle (θ) of 90°. The suggested design exhibits good absorption bandwidth, with absorptivity greater than 90% even at an incidence angle of 45° as shown in Fig. 6.

Aside from the oblique incidence angle (θ), the absorption characteristics of different polarization angles (φ) ranging from 0 to 90° are also investigated for sample RHC-11 when the incidence angle is normal, ensuring that the wave propagates in the direction parallel to the *z*-axis. The simulated result for this is shown in Fig. 7, where the suggested structure is shown to be completely insensitive to polarization angle variation. The absorption curve pattern follows the same pattern for all the angle variations, from 0 to 90^{0}, as shown in Fig. 7. This insensitiveness of the proposed design result is due to the symmetrical patch design.

The features of the suggested microwave absorber were also compared with recently published absorbers studied by various researchers to accurately define the performance of the suggested microwave absorber in comparison to the state-of-the-art, with a focus on thickness, materials used, and absorption bandwidth. The material used in the comparison table is mostly FR4 as the main substrate with varying thicknesses. As seen in Table 6, all the parameters such as the material used, thickness, and bandwidth have been compared. Furthermore, the suggested absorber has several benefits, including less polarization impact, lower thickness, and the broader absorption bandwidth, making it a good contender for possible applications, especially operating in the K_u band.

6 Conclusion

To investigate the microwave absorption properties, waste materials such as rice husk and exhausted activated carbon with a composition of EAC ranging from 0 to 30% by weight were used to manufacture samples using a simple mechanical approach such as cleaning, drying, milling, and compaction.

Table 6 Comparison between reference absorbers and proposed absorber

S. no	Substrate	Thickness (mm)	Bandwidth with absorptivity > 90%	Frequency and absorption	Reference
1	A4 copy paper	7.2	0.4 GHz	6.7–7.1 GHz > 90%	10
2	FR-4	2.4	< 2 GHz	5.4 GHz, 7.6 GHZ, 12.4 GHz > 90%	14
3	FR-4	2.4	< 4 GHz	5.3 GHz, 7.9 GHz, 13.6 GHz > 90%	15
4	F_4B-2	3	3.8 GHz	9.1–12.9 GHz > 90%	13
5	Al Fe_3O_4-Ti	3.4	4.2 GHz	8.4–12.4 GHz > 90%	12
6	FR4	4.5	4.2 GHz	7–11.2 GHz > 90%	26
7	MAM	3.5	< 4 GHz	6 GHz > 90%	26
8	PET FeCoB	3	5.08 GHz	9.99–15.07 GHz > 90%	27
9	FR-4	5	2.46 GHz	2.85–5.31 GHz > 90%	11
10	FR 4	2	1.62 GHz	7.18–8.8 GHz > 90%	28
11	RHC FR 4	2.3	6.61 GHz	12.16–18.76 GHz > 90%	Present work

At various thicknesses, the sample displayed a fair reflection loss peak in samples RHC-9 to RHC-13. Sample RHC-11 at a thickness of 14 mm had the best reflection loss peak of − 38.3 dB at a frequency of 12 GHz, indicating that it has good potential for use in an anechoic chamber. The samples' dielectric properties were also exploited to produce a superior microwave absorber in the form of a metamaterial. A design has been proposed that incorporates copper, RHC samples, FR4 epoxy as a substrate, and patches using resistive ink. With RHC-11 at a thickness of 2.3 mm, the proposed design demonstrated good microwave absorption (absorptivity greater than 0.9) with a broader bandwidth of 6.61 GHz from 12.16 to 18.76 GHz. At 16 GHz, the maximum absorptivity was 99.34%, and the bandwidth with an absorptivity greater than 0.95 was 4.02 GHz between 13.38 and 17.40 GHz.

Acknowledgements The first author wants to thank MHRD, India, for providing fund to carry out the research work and also thanks to Centre of Interdisciplinary Research (CIR), MNNIT Allahabad for carrying out the characterization process. The author expresses their gratitude to DMSRDE Kanpur for getting the sample tested by Vector Network Analyzer (VNA).

Author Contribution Deeksha Gupta: methodology, validation, investigation, and formal analysis. Prabhakar Kumar: investigation. Ashish Dubey: supervision, writing—review and editing. Abhishek Kumar: conceptualization, funding acquisition, supervision, and writing—review and editing.

Data Availability All the data related to the article is available in the manuscript itself.

Declarations

Conflict of Interest The authors declare no competing interests.

References

1. Z. Wu, Z. Meng, C. Yao, Y. Deng, G. Zhang, Y. Wang, Rice husk derived hierarchical porous carbon with lightweight and efficient microwave absorption. Mater. Chem. Phys. **275**, (2022). https://doi.org/10.1016/j.matchemphys.2021.125246
2. J. Ouyang, Z. He, Y. Zhang, H. Yang, Q. Zhao, A.C.S. Appl, Mater. Interfaces **11**, 39304 (2019)
3. Y. Wang, X. Gao, H. Zhou, X. Wu, W. Zhang, Q. Wang, C. Luo, Powder Technol. **345**, 370 (2019)
4. T. Liu, N. Liu, L. Gai, Q. An, Z. Xiao, S. Zhai, W. Cai, H. Wang, Z. Li, Microporous Mesoporous Mater. **302**, 110210 (2020)
5. X. Qiu, L. Wang, H. Zhu, Y. Guan, Q. Zhang, Nanoscale **9**, 7408 (2017)
6. P. Negi, A. K. Chhantyal, A. K. Dixit, S. Kumar, A. Kumar, Activated carbon derived from mango leaves as an enhanced microwave absorbing material. Sustain. Mater. Technol. **27**, (2021). https://doi.org/10.1016/j.susmat.2020.e00244
7. S.P. Mishra, G. Nath, P. Mishra, Mater. Today Proc. **24**, 585 (2020)
8. Y.S. Lee, F. Malek, E.M. Cheng, W.W. Li, F.H. Wee, M.N. Iqbal, L. Zahid, F. Abdullah, A.Z. Abdullah, N.S. Noorpi, N.M. Mokhtar, M.A. Jusoh, Lect. Notes Electr. Eng. **344**, 41 (2015)
9. J.N. Hwang, F.C. Chen, IEEE Trans. Antennas Propag. **54**, 3763 (2006)
10. M. Momeni-Nasab, S.M. Bidoki, M. Hadizadeh, M. Movahhedi, AEU - Int. J. Electron. Commun. **123**, 153259 (2020)
11. W. Yuan, Y. Cheng, Appl. Phys. A Mater. Sci. Process. **117**, 1915 (2014)
12. R. Panwar, S. Puthucheri, V. Agarwala, D. Singh, IEEE Trans. Microw. Theory Tech. **63**, 2438 (2015)
13. H. Y. Chen, J. F. Wang, H. Ma, S. B. Qu, J. Q. Zhang, Z. Xu, A. X. Zhang, Broadband perfect polarization conversion metasurfaces. Chinese Phys. B **24**, (2015). https://doi.org/10.1088/1674-1056/24/1/014201
14. M. I. Khan, F. A. Tahir, A broadband cross-polarization conversion anisotropic metasurface based on multiple plasmon resonances. Chinese Phys. B **27**, (2018). https://doi.org/10.1088/1674-1056/27/1/014101
15. M. I. Khan, Q. Fraz, F. A. Tahir, Ultra-wideband cross polarization conversion metasurface insensitive to incidence angle. J. Appl. Phys. **121**, (2017). https://doi.org/10.1063/1.4974849
16. L. Feng, W. Li, Y. Wang, J. Magn. Magn. Mater. **541**, 168510 (2022)
17. Y. Hussain, R. Baqir, A. Anam, Ultrathin graphene metasurface-based microwave absorber. engrxiv.org. (2022). https://doi.org/10.31224/2549
18. A.K. Saurabh, S. Singh. Maurya, A. Kumar, Def. Sci. J. **69**, 437 (2019)
19. S. Singh, A. Sinha, R.H. Zunke, A. Kumar, D. Singh, Adv. Powder Technol. **29**, 2019 (2018)
20. S. Singh, S. Shukla, A. Kumar, D. Singh, J. Alloys Compd. **738**, 448 (2018)
21. Y. Wei, H. Liu, S. Liu, M. Zhang, Y. Shi, J. Zhang, L. Zhang, C. Gong, Compos. Commun. **9**, 70 (2018)
22. S. Singh, A. Kumar, D. Singh, J. Electron. Mater. **49**, 7279 (2020)
23. A. Saptarshi Ghosh, Somak Bhattacharyya and K. V. Srivastava, Microw. Opt. Technol. Lett. **56**, 350 (2014)
24. H.S. Singh, Microw. Opt. Technol. Lett. **62**, 718 (2020)
25. Y. Tayde, M. Saikia, K.V. Srivastava, S.A. Ramakrishna, IEEE Antennas Wirel. Propag. Lett. **17**, 2489 (2018)
26. Z. Liao, R. Gong, Y. Nie, T. Wang, X. Wang, Absorption enhancement of fractal frequency selective surface absorbers by using microwave absorbing material based substrates. Photonics Nanostruct. Fundam. Appl. **9**, 287–294 (2011). https://doi.org/10.1016/j.photonics.2011.05.006
27. W. Ren, Y. Nie, X. Xiong, C. Zhang, Y. Zhou, R. Gong, Enhancing and broadening absorption properties of frequency selective surfaces absorbers using FeCoB-based thin film. J. Appl. Phys. **111**, (2012). https://doi.org/10.1063/1.3670980
28. Y. Cheng, H. Luo, F. Chen, Broadband metamaterial microwave absorber based on asymmetric sectional resonator structures. J. Appl. Phys. **127**, (2020). https://doi.org/10.1063/5.0002931